X 68 18887

~~CONFIDENTIAL~~

NASA TECHNICAL MEMORANDUM

UB
NASA TM X-1610

UB
NASA TM X-1610

CLASSIFICATION CHANGE

To UNCLASSIFIED
By authority of GDS-E.O. 11652
Changed by O. C. Pendergraft Date 12/31/74
Classified Document Master Control Station, NASA
Scientific and Technical Information Facility

NOFORN

EFFECT OF CAMBER AND TWIST ON LONGITUDINAL AERODYNAMIC CHARACTERISTICS OF A WING-FUSELAGE MODEL AT MACH NUMBERS UP TO 1.30

by Odis C. Pendergraft, Jr.

Langley Research Center
Langley Station, Hampton, Va.

NATIONAL AERONAUTICS AND SPACE ADMINISTRATION • WASHINGTON, D. C. • AUGUST 1968

~~CONFIDENTIAL~~

~~CONFIDENTIAL~~

NASA TM X-1610

~~CLASSIFIED DOCUMENT~~
SUBJECT TO GENERAL DECLASSIFICATION
SCHEDULE OF EXECUTIVE ORDER 11652.
AUTOMATICALLY DOWNGRADED AT
TWO-YEAR INTERVALS.
DECLASSIFIED ON DECEMBER 31, 1974

EFFECT OF CAMBER AND TWIST ON LONGITUDINAL AERODYNAMIC CHARACTERISTICS OF A WING-FUSELAGE MODEL AT MACH NUMBERS UP TO 1.30

By Odis C. Pendergraft, Jr.

Langley Research Center
Langley Station, Hampton, Va.

~~NOFORN~~

~~GROUP 4~~
~~Downgraded at 12 year intervals;~~
~~declassified after 12 years~~

~~CLASSIFIED DOCUMENT-TITLE UNCLASSIFIED~~
~~This material contains information affecting the national defense of the United States within the meaning of the espionage laws, Title 18, U.S.C., Secs. 793 and 794, the transmission or revelation of which in any manner to an unauthorized person is prohibited by law.~~

NOTICE
This document should not be returned after it has satisfied your requirements. It may be disposed of in accordance with your local security regulations or the appropriate provisions of the Industrial Security Manual for Safe-Guarding Classified Information.

NATIONAL AERONAUTICS AND SPACE ADMINISTRATION

~~CONFIDENTIAL~~

CONFIDENTIAL

EFFECT OF CAMBER AND TWIST ON LONGITUDINAL AERODYNAMIC CHARACTERISTICS OF A WING-FUSELAGE MODEL AT MACH NUMBERS UP TO 1.30*

By Odis C. Pendergraft, Jr.
Langley Research Center

SUMMARY

The longitudinal aerodynamic characteristics of two 75° sweptback wing-fuselage models, one having a symmetrical wing of aspect ratio 1.61 and the other having a wing with the same planform and thickness distribution but with camber and twist (8.5° washout at the tip), were determined in the Langley 16-foot transonic tunnel at Mach numbers from 0.30 to 1.30 and angles of attack from about -2° to 11°.

The configuration with the cambered and twisted wing had slightly higher minimum drag than the symmetrical-wing configuration but also had higher lift-drag ratios and, over the Mach number range, achieved lift coefficients about 0.05 to 0.075 higher before longitudinal instability occurred. The performance gains of the cambered-and-twisted-wing configuration over the symmetrical-wing configuration may be attributed primarily to improved span load efficiency.

INTRODUCTION

Large military aircraft designed to cruise at high altitudes and Mach numbers must also operate efficiently at subsonic and transonic speeds at lower altitudes. Special requirements such as subsonic cruise (to obtain maximum range) or low-level supersonic dash (to avoid radar detection) make optimum performance at these conditions equally as important as performance at high Mach number cruise conditions.

The purpose of this investigation was to determine the effects of camber and twist on the subsonic and transonic longitudinal aerodynamic characteristics of a wing-body configuration with low wings. The models used simulated bomber aircraft designed to cruise at a Mach number of 3.0. The separate effects of the leading-edge-suction and span-load-efficiency parameters on performance were isolated by a method presented in reference 1. Each model had a planform aspect ratio of 1.61, a leading-edge sweep angle

*Title, Unclassified.

CONFIDENTIAL

of 75°, a constant spanwise thickness-chord ratio of 0.025, a modified NACA 65A-series airfoil section, and a cylindrical fuselage with an ogive nose.

In this investigation, which was conducted in the Langley 16-foot transonic tunnel, the Mach number was varied from 0.30 to 1.30 and angles of attack ranged from about -2° to 11°. The test Reynolds number per meter varied from 6.2×10^6 to 13.3×10^6.

SYMBOLS

A	aspect ratio of wing $\left(\frac{b^2}{S} = 1.61\right)$
A_m	model cross-sectional area, meters^2
b	wing span, meters
c	streamwise local chord, meters
$\bar{c}$	streamwise mean aerodynamic chord, meters
C_D	drag coefficient, $\frac{\text{Drag}}{qS}$
$C_{D,f}$	skin-friction drag coefficient
$C_{D,min}$	minimum drag coefficient
$C_{D,o}$	drag coefficient at zero lift for symmetrical wing
$C_{D,W}$	wave-drag coefficient
$C_{D,2}$	minimum drag coefficient for cambered wing (called $C_{D,M}$ in ref. 1)
C_L	lift coefficient, $\frac{\text{Lift}}{qS}$
$C_{L,2}$	lift coefficient at $C_{D,2}$ (called $C_{L,M}$ in ref. 1)
C_{L_α}	lift-curve slope per degree, $\left(\frac{\partial C_L}{\partial \alpha}\right)_{C_L \approx 0}$
C_m	pitching-moment coefficient, $\frac{\text{Pitching moment}}{qS\bar{c}}$

$C_{m_{C_L}}$ longitudinal-stability parameter measured at $C_L = 0$

$C_{p,b}$ base pressure coefficient, $\frac{p_b - p_\infty}{q}$

k_1 drag-due-to-lift factor for symmetrical wing, $\frac{dC_D}{dC_L^2}$ (called k_A in ref. 1)

k_2 drag-due-to-lift factor for cambered and twisted wing, $\frac{\partial C_D}{\partial (C_L - C_{L,2})^2}$ (called k_M in ref. 1)

$k_{2,min}$ minimum drag-due-to-lift factor for cambered and twisted wing

l maximum body length (88.798 centimeters)

L/D lift-drag ratio

$(L/D)_{max}$ maximum lift-drag ratio

M free-stream Mach number

p_b base pressure, newtons/meter^2

p_∞ free-stream static pressure, newtons/meter^2

q free-stream dynamic pressure, newtons/meter^2

r leading-edge radius of wing, meters

S total wing area (0.0836 meter^2)

t wing thickness, meters

x longitudinal wing ordinate measured in axial direction (positive downstream), meters

x' longitudinal body ordinate measured from tip of nose (positive rearward), meters

y spanwise station, meters

z_l, z_u wing ordinates for lower and upper surfaces, respectively, measured perpendicular to wing reference plane (positive up), meters

α angle of attack of body center line, degrees

APPARATUS AND PROCEDURE

Model

A sketch of the symmetrical-wing model (designated configuration 1) is shown in figure 1(a), and a sketch of the cambered-and-twisted-wing model (designated configuration 2) is shown in figure 1(b). Photographs of these models mounted in the test section of the Langley 16-foot transonic tunnel are presented as figure 2, and the model cross-sectional-area distribution is shown in figure 3.

Wings.- The wings of both configurations had a planform aspect ratio of 1.61, a leading-edge sweep angle of 75°, a constant spanwise thickness-chord ratio of 0.025, and a modified NACA 65A-series airfoil section. Configuration 1 had symmetrical airfoil sections with no twist, whereas the wing of configuration 2 was designed with camber and twist (8.5° washout at spanwise station 16.51 – see fig. 1(b)) for a lift coefficient of 0.10 at $M = 3.0$. Airfoil ordinates for three spanwise stations for the symmetrical wing and six spanwise stations for the cambered and twisted wing are given in table I. These ordinates are referred to the wing reference plane shown in figure 1(a) for the symmetrical wing and in figure 1(b) for the cambered wing. Because of the wing camber of configuration 2, its root chord line was located 0.115 cm lower than the root chord of configuration 1. Boundary-layer transition strips were located 0.254 cm from the leading edge on both upper and lower surfaces of the wing and were 0.20 cm wide. (No. 80 carborundum grit was used, and 12 to 16 grains were applied per centimeter of length.)

Fuselage.- The fuselage was symmetrical about the body axis and consisted of two parts. The nose piece was an ogive 27.076 cm long with a maximum diameter of 4.724 cm. The cylindrical afterbody had the same diameter and was 61.722 cm long. The same size and type of transition strip used on the wing was also used on the fuselage, except the transition strip on the fuselage was located around the nose 2.54 cm downstream.

Wind Tunnel and Instrumentation

This investigation was conducted in the Langley 16-foot transonic tunnel, which is of the single-return, continuous-flow type having an octagonal slotted test section measuring 4.7 meters across the flats. The tunnel is operated at atmospheric stagnation pressures and is capable of attaining a Mach number of 1.3 with the aid of a compressor

system which draws air out through the test-section slots. A description of the tunnel is in reference 2. The model was sting mounted on a support strut, and the sting-support system was designed to keep the model close to the tunnel center line throughout the angle-of-attack range.

Forces and moments on the model were measured by an internally located, six-component, strain-gage balance. Model angle of attack was determined by measuring the sting angle and adding the sting and model deflections. Base pressure of the model was measured by means of an electrical pressure transducer which was connected to two manifolded pressure orifices located 180° apart in the open annulus between the sting and fuselage inner surface about 0.5 cm ahead of the model base.

Tests and Corrections

The model was tested at Mach numbers from 0.30 to 1.30 and angles of attack from about -2° to 11°. The test Reynolds number per meter varied from 6.2×10^6 to 13.3×10^6. Tests were conducted on the symmetrical model in both upright and inverted positions to determine the tunnel flow angularities.

Model forces were adjusted to the condition corresponding to free-stream static pressure at the base of the model. For $M = 1.05$ this correction amounted to about 25 percent of the total model drag of configuration 1. The model base area was 17.52 cm^2. Base pressure coefficients for both configurations are presented in figure 4. The drag coefficients were corrected for tunnel buoyancy effects and the corrections vary from 0 to 0.00017, depending on Mach number. The angle of attack was corrected for balance and sting deflections due to model aerodynamic loads and for wind-tunnel flow angularities. No other corrections were made.

RESULTS AND DISCUSSION

Basic Characteristic

The basic longitudinal aerodynamic characteristics for the two configurations are presented in figure 5. Both configurations exhibit nonlinear pitching-moment curves over the entire Mach number range, but the symmetrical wing (configuration 1) shows unstable tendencies at values of C_L approximately 0.05 to 0.075 lower than those for the cambered and twisted wing (configuration 2). The improved stability of configuration 2 can be attributed to wing-tip washout created by twisting the wing. The lift curves appear to have the same overall slope, but because of nonlinearities in the curves, the slopes are different near $C_L = 0$. The drag polars exhibit the expected trends for the two configurations, with the cambered wing generally having the higher minimum drag

but having lower drag than the symmetrical wing for values of C_L greater than 0.03 to 0.09, depending on Mach number.

Summary Data

The summary data for $(L/D)_{max}$, C_L for $(L/D)_{max}$, Cm_{C_L}, and C_{L_α} are presented as a function of Mach number in figure 6. For the symmetrical wing (configuration 1), $(L/D)_{max}$ increased smoothly from 6.6 at $M = 0.30$ to a maximum of 8.0 at $M = 1.30$ with only a slight irregularity around $M = 1.0$. For the cambered wing (configuration 2), the values of $(L/D)_{max}$ were always higher than those for the symmetrical wing, as expected, and varied from 9.3 at $M = 0.30$ to a maximum of 9.9 at $M = 0.90$. At this point, a noticeable decrease occurred in the transonic region; that is, the value of $(L/D)_{max}$ decreased to about 9.0 at $M = 1.10$ and then increased slightly and held nearly constant at 9.4 to $M = 1.30$. The variation of C_L for $(L/D)_{max}$ with Mach number is approximately constant for both configurations. A comparison of C_m for the two configurations (fig. 5) at $C_L = 0.15$ $\left(\text{near } (L/D)_{max}\right)$ indicates that the maximum trimmed L/D would be higher for the cambered wing. Comparison of the static margin Cm_{C_L} for the two configurations indicates that the cambered wing had a nearly constant higher increment of static stability than the symmetrical wing over the Mach number range. The lift-curve slope at $C_L \approx 0$ is higher for the cambered wing than for the symmetrical wing over the entire Mach number range.

Drag Characteristics

A comparison of measured minimum drag for both configurations is presented in figure 7. Also presented are the computed skin-friction drag and the computed skin-friction drag plus wave drag for the symmetrical wing (configuration 1). Skin-friction drag (assuming a fully turbulent boundary layer) was computed by the T' method (ref. 3) with the aid of the simplified procedure given in reference 4, and wave drag was computed by using the methods of reference 5. Except at $M = 0.30$, where the low values of q produce relatively poor accuracies, $C_{D,min}$ is always lower for the symmetrical-wing configuration than for the cambered-wing configuration; for both configurations the transonic drag rise begins at about $M = 0.95$ and peaks near $M = 1.08$. Good agreement exists between measured $C_{D,min}$ and computed $C_{D,f} + C_{D,W}$.

Effects of Leading-Edge Suction and Span Load Efficiency on Performance

Although the evaluation of the relative performance of the two configurations was the prime objective of the investigation, the similar geometry of the two wings presented an excellent opportunity to determine the effect of the leading-edge-suction and

span-load-efficiency parameters on performance. The method presented in reference 1 was used to isolate the effects of each parameter.

The lift-drag ratios measured for the cambered wing were greater than those for the symmetrical wing, a result which may be attributed to an improvement in the cambered-wing drag-due-to-lift factor. Two important contributions to this factor are the wing span load efficiency and the wing leading-edge suction. To determine the relative importance of these contributions to improved wing performance, the drag polars for the symmetrical- and the cambered-wing configurations were examined. The drag polars were fitted with equations of the following form:

For the symmetrical wing,

$$C_D = C_{D,o} + k_1 C_L^2 \tag{1}$$

and for the cambered and twisted wing,

$$C_D = C_{D,2} + k_2 (C_L - C_{L,2})^2 \tag{2}$$

By fitting the drag polars in this manner, the values of k_1 in equation (1) and k_2 in equation (2) were determined. However, if an equation similar to equation (1) is fitted to the drag polars for the cambered wing, then the drag-due-to-lift factor (k_1 in eq. (1)) is no longer constant (as it was for the symmetrical wing) but varies from infinity for $C_L = 0$ to some minimum value. This minimum drag-due-to-lift factor for configuration 2 is designated $k_{2,min}$.

As explained in the appendix of reference 1, a comparison of k_1 for the symmetrical wing with k_2 for the cambered wing shows the relative effects of leading-edge suction on the drag-due-to-lift factor, and a comparison of k_2 and $k_{2,min}$ for the cambered wing shows the relative effects of wing span load efficiency. The drag-due-to-lift factors (k_1 for the symmetrical wing and k_2 and $k_{2,min}$ for the cambered wing) multiplied by the aspect ratio A are presented as functions of Mach number in figure 8. The full-suction and no-suction boundaries for the two configurations are also included in figure 8 for comparison.

At all Mach numbers, the cambered-wing drag-due-to-lift factor is primarily improved (as indicated in fig. 8 by the much lower values for $k_{2,min}A$ in comparison with those for k_2A) because the cambered and twisted wing attained much better span load efficiency than the symmetrical wing – a direct result of the twisted wing surfaces. Between $M = 1.00$ and 1.20 this improvement is somewhat degraded, but the span load efficiency is still the most significant parameter in improving the wing performance. It is also evident that wing camber did not significantly improve the leading-edge suction, as indicated by the small difference between k_1A and k_2A.

CONCLUSIONS

An investigation to determine the aerodynamic characteristics of two 75° sweptback wing-fuselage models, one having a symmetrical wing and the other having a wing with the same planform and thickness distribution but with camber and twist (8.5° washout at the tip), has been conducted at Mach numbers from 0.30 to 1.30 and angles of attack from about -2° to 11°. Results of the investigation indicate the following conclusions:

1. Because of the wing-tip washout created by twisting the wing, longitudinal instability was delayed for the cambered-and-twisted-wing configuration, as shown by the fact that the lift coefficients were about 0.05 to 0.075 higher than those for the symmetrical-wing configuration.

2. The cambered-and-twisted-wing configuration had the higher minimum drag, but had lower drag than the symmetrical-wing configuration for values of lift coefficient greater than 0.03 to 0.09, depending on Mach number.

3. The cambered and twisted wing had a nearly constant higher increment of static stability than the symmetrical wing over the Mach number range.

4. Good agreement was found between the measured minimum drag and the computed skin-friction drag plus wave drag for the symmetrical-wing configuration.

5. Little difference was apparent in the leading-edge-suction parameters of the two configurations, but the cambered and twisted wing attained much better span load efficiency than the symmetrical wing.

Langley Research Center,
National Aeronautics and Space Administration,
Langley Station, Hampton, Va., January 24, 1968,
720-01-00-12-23.

REFERENCES

1. Igoe, William B.; Re, Richard J.; and Cassetti, Marlowe D.: Transonic Aerodynamic Characteristics of a Wing-Body Combination Having a 52.5° Sweptback Wing of Aspect Ratio 3 With Conical Camber and Designed for a Mach Number of $\sqrt{2}$. NASA TN D-817, 1961.

2. Ward, Vernon G.; Whitcomb, Charles F.; and Pearson, Merwin D.: Air-Flow and Power Characteristics of the Langley 16-Foot Transonic Tunnel With Slotted Test Section. NACA RM L52E01, 1952.

3. Sommer, Simon C.; and Short, Barbara J.: Free-Flight Measurements of Turbulent-Boundary-Layer Skin Friction in the Presence of Severe Aerodynamic Heating at Mach Numbers From 2.8 to 7.0. NACA TN 3391, 1955.

4. Peterson, John B., Jr.: A Comparison of Experimental and Theoretical Results for the Compressible Turbulent-Boundary-Layer Skin Friction With Zero Pressure Gradient. NASA TN D-1795, 1963.

5. Harris, Roy V., Jr.: An Analysis and Correlation of Aircraft Wave Drag. NASA TM X-947, 1964.

TABLE I.- WING ORDINATES

(a) Configuration 1

x/c	y = 1.905 cm (c = 33.919 cm; r = 0.0686 cm)		y = 14.188 cm (c = 17.351 cm; r = 0.0356 cm)		y = 16.510 cm (c = 7.694 cm; r = 0.0152 cm)	
	z_u/c	z_l/c	z_u/c	z_l/c	z_u/c	z_l/c
0	0	0	0	0	0	0
.0125	.0030	-.0030	.0029	-.0029	.0030	-.0030
.0250	.0040	-.0040	.0038	-.0038	.0040	-.0040
.0500	.0055	-.0055	.0053	-.0053	.0056	-.0056
.0750	.0066	-.0066	.0064	-.0064	.0066	-.0066
.1000	.0076	-.0076	.0073	-.0073	.0076	-.0076
.1500	.0091	-.0091	.0088	-.0088	.0092	-.0092
.2000	.0103	-.0103	.0100	-.0100	.0106	-.0106
.2500	.0112	-.0112	.0108	-.0108	.0116	-.0116
.3000	.0119	-.0119	.0116	-.0116	.0122	-.0122
.4000	.0126	-.0126	.0122	-.0122	.0129	-.0129
.5000	.0122	-.0122	.0119	-.0119	.0125	-.0125
.6000	.0109	-.0109	.0105	-.0105	.0112	-.0112
.7000	.0087	-.0087	.0085	-.0085	.0092	-.0092
.8000	.0060	-.0060	.0059	-.0059	.0063	-.0063
.9000	.0031	-.0031	.0031	-.0031	.0036	-.0036
1.0000	.0001	-.0001	.0003	-.0003	.0007	-.0007

TABLE I.- WING ORDINATES – Concluded

(b) Configuration 2

x/c	y = 1.905 cm (c = 33.919 cm; r = 0.0686 cm)		y = 3.810 cm (c = 31.351 cm; r = 0.0635 cm)		y = 6.350 cm (c = 27.924 cm; r = 0.0559 cm)		y = 9.180 cm (c = 24.107 cm; r = 0.0483 cm)		y = 14.188 cm (c = 17.351 cm; r = 0.0356 cm)		y = 16.510 cm (c = 7.694 cm; r = 0.0152 cm)	
	z_u/c	z_l/c	z_u/c	z_l/c	z_u/c	z_l/c	z_u/c	z_l/c	z_u/c	z_l/c	z_u/c	z_l/c
0	0.0310	0.0310	0.0178	0.0178	0.0091	0.0091	0.0024	0.0024	-0.0064	-0.0064	-0.0165	-0.0165
.0125	.0341	.0282	.0211	.0151	.0125	.0065	.0059	0	-.0029	-.0086	-.0125	-.0185
.0250	.0352	.0273	.0224	.0144	.0139	.0060	.0075	-.0004	-.0012	-.0088	-.0106	-.0185
.0500	.0367	.0258	.0242	.0134	.0161	.0052	.0100	-.0009	.0016	-.0089	-.0073	-.0182
.0750	.0373	.0240	.0254	.0121	.0175	.0044	.0117	-.0016	.0037	-.0092	-.0046	-.0182
.1000	.0374	.0222	.0259	.0108	.0185	.0034	.0131	-.0022	.0053	-.0095	-.0026	-.0178
.1500	.0366	.0183	.0265	.0082	.0198	.0015	.0149	-.0035	.0079	-.0098	.0013	-.0172
.2000	.0350	.0143	.0261	.0053	.0203	-.0005	.0159	-.0048	.0097	-.0102	.0043	-.0168
.2500	.0326	.0101	.0250	.0025	.0201	-.0025	.0163	-.0062	.0111	-.0107	.0066	-.0162
.3000	.0297	.0058	.0235	-.0004	.0195	-.0045	.0164	-.0075	.0120	-.0110	.0086	-.0155
.4000	.0219	-.0032	.0188	-.0064	.0167	-.0085	.0152	-.0100	.0127	-.0117	.0112	-.0145
.5000	.0123	-.0122	.0122	-.0122	.0122	-.0122	.0122	-.0122	.0119	-.0119	.0125	-.0125
.6000	.0007	-.0212	.0041	-.0178	.0062	-.0156	.0078	-.0141	.0095	-.0116	.0122	-.0102
.7000	-.0124	-.0300	-.0058	-.0232	-.0014	-.0188	.0019	-.0157	.0061	-.0108	.0109	-.0073
.8000	-.0270	-.0390	-.0167	-.0288	-.0098	-.0219	-.0050	-.0171	.0018	-.0101	.0086	-.0043
.9000	-.0422	-.0485	-.0283	-.0345	-.0190	-.0254	-.0122	-.0186	-.0031	-.0094	.0059	-.0013
1.0000	-.0580	-.0583	-.0405	-.0408	-.0287	-.0291	-.0201	-.0206	-.0082	-.0088	.0026	.0013

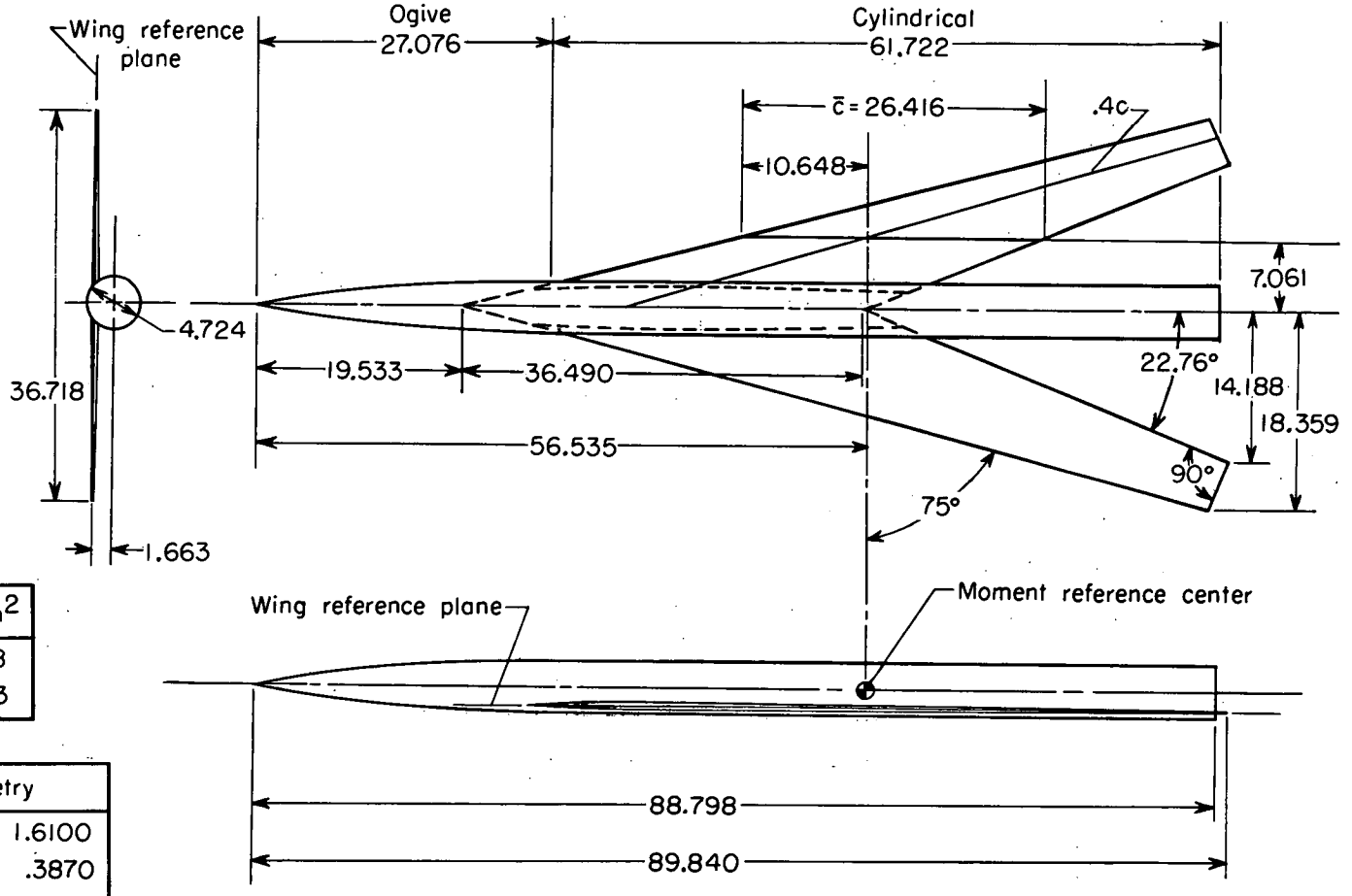

Wetted areas, m^2	
Fuselage	.1058
Wing	.1443

Wing geometry	
Aspect ratio	1.6100
Taper ratio	.3870
Wing area, m^2	.0836
t/c	.0250
Airfoil section	*

* Modified NACA 65A-series, see table I.

(a) Configuration 1 (symmetrical-wing model).

Figure 1.- Sketches of models. All dimensions are in centimeters.

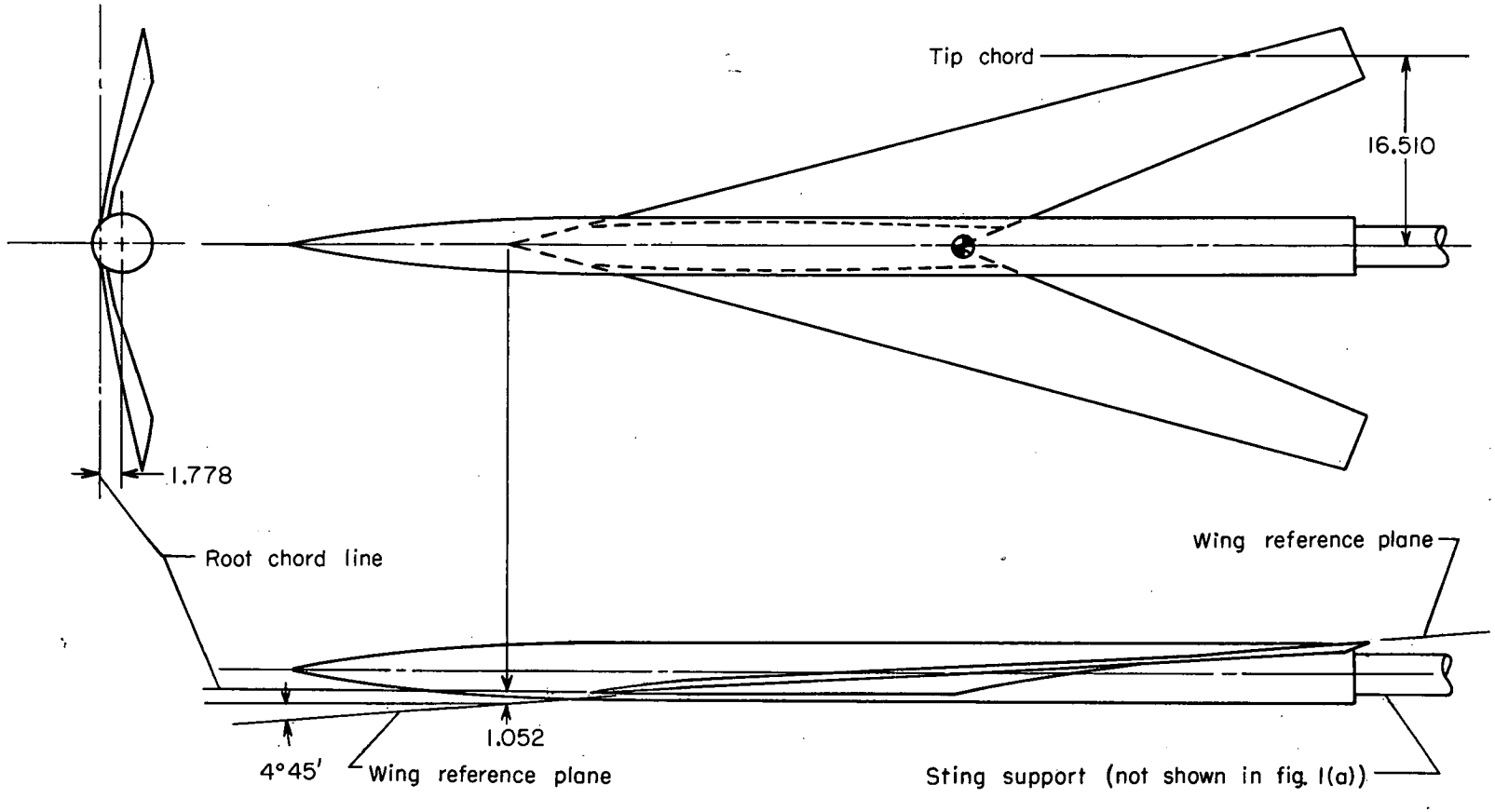

(b) Configuration 2 (cambered-and-twisted-wing model). All dimensions, except as noted, are identical to those of configuration 1.

Figure 1.- Concluded.

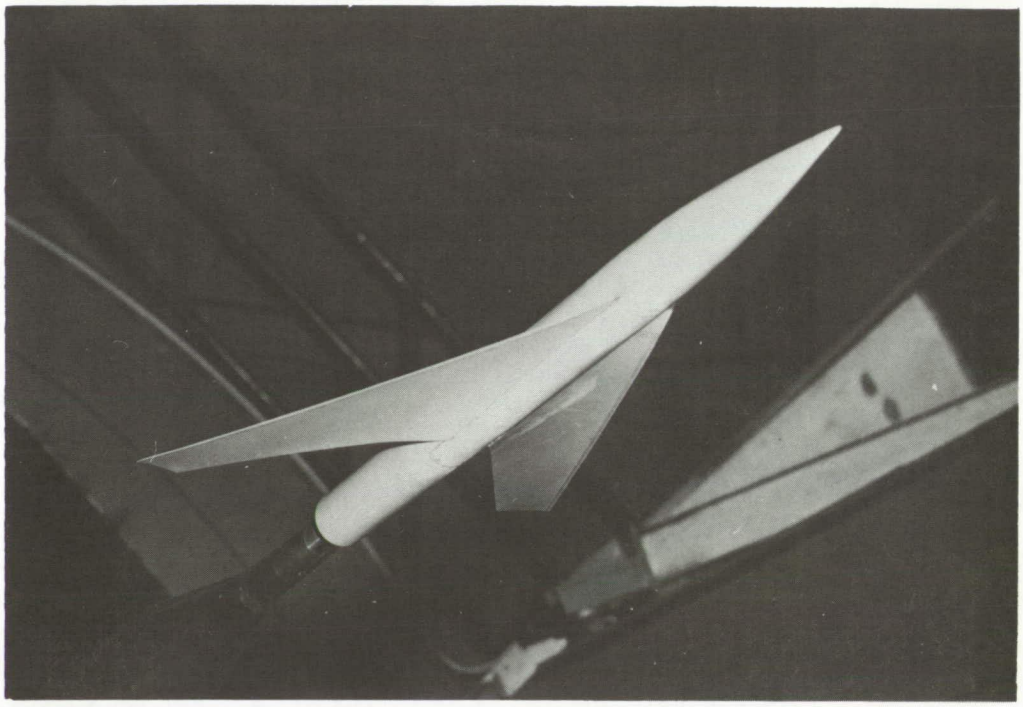

Cambered-wing model L-64-857

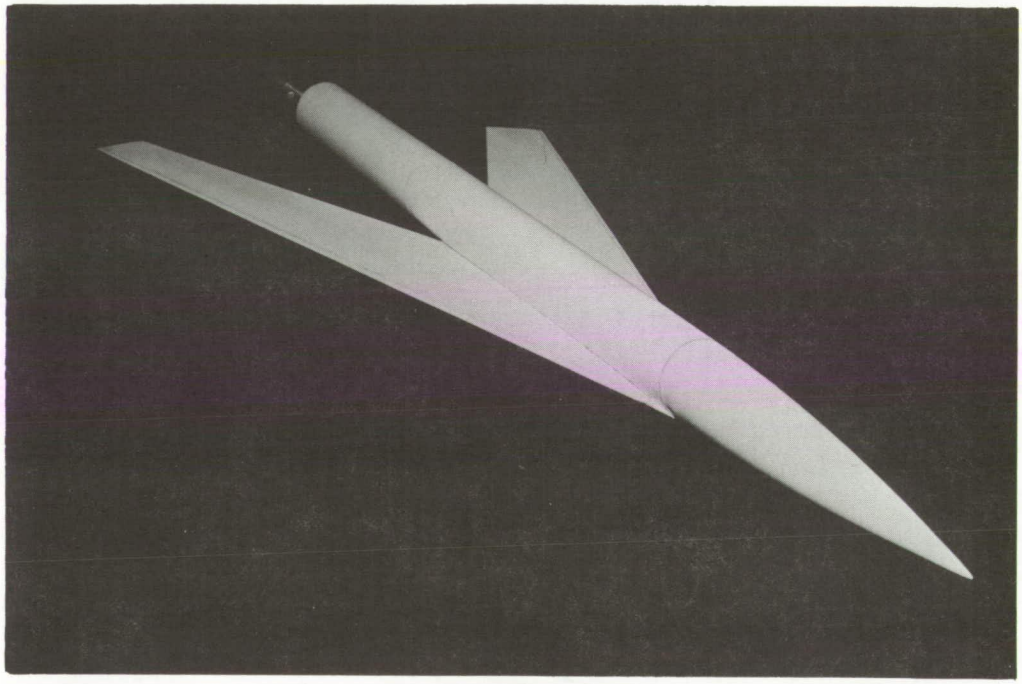

Symmetrical-wing model

Figure 2.- Photographs of models installed in test section. L-64-733

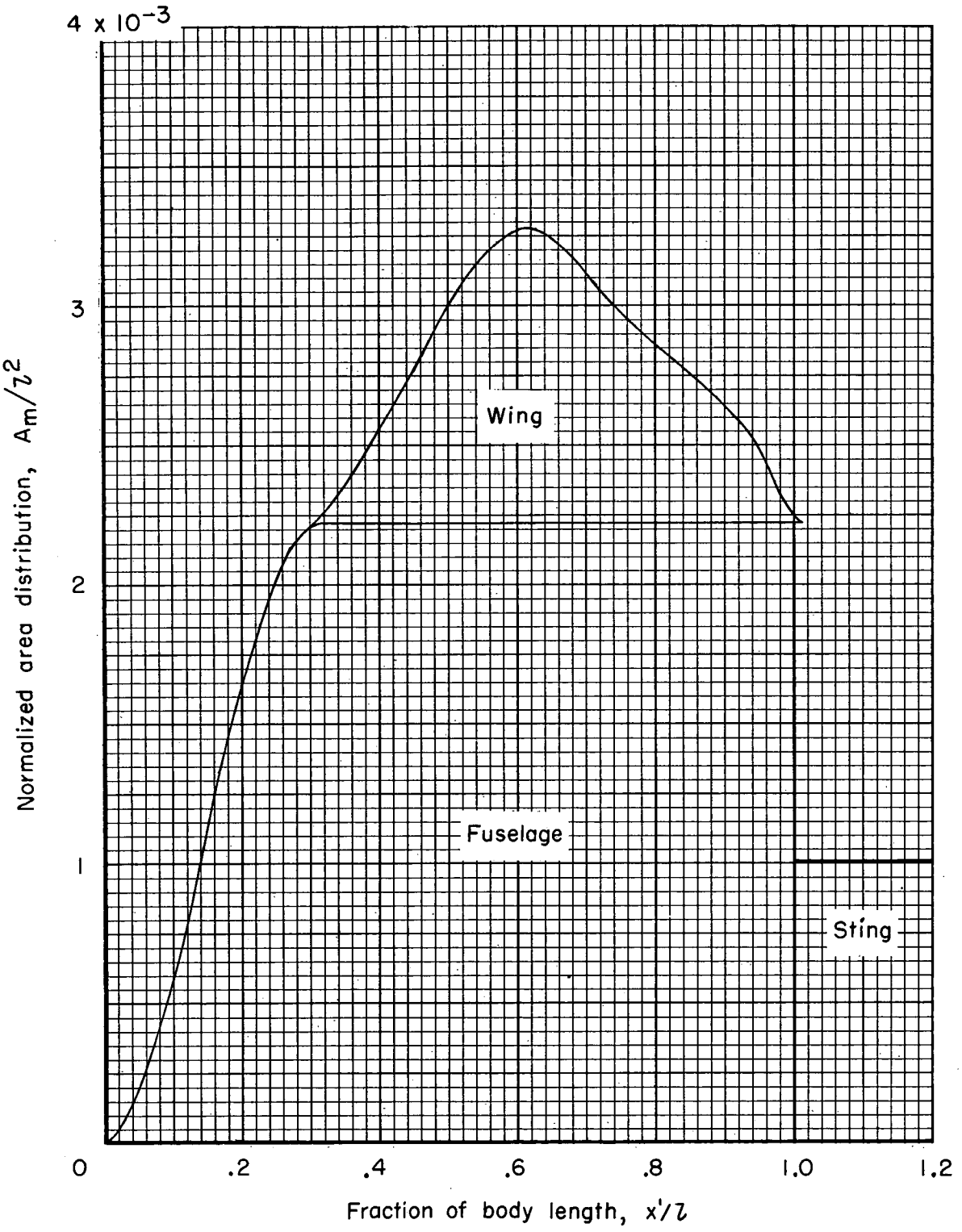

Figure 3.- Cross-sectional-area distribution of model.

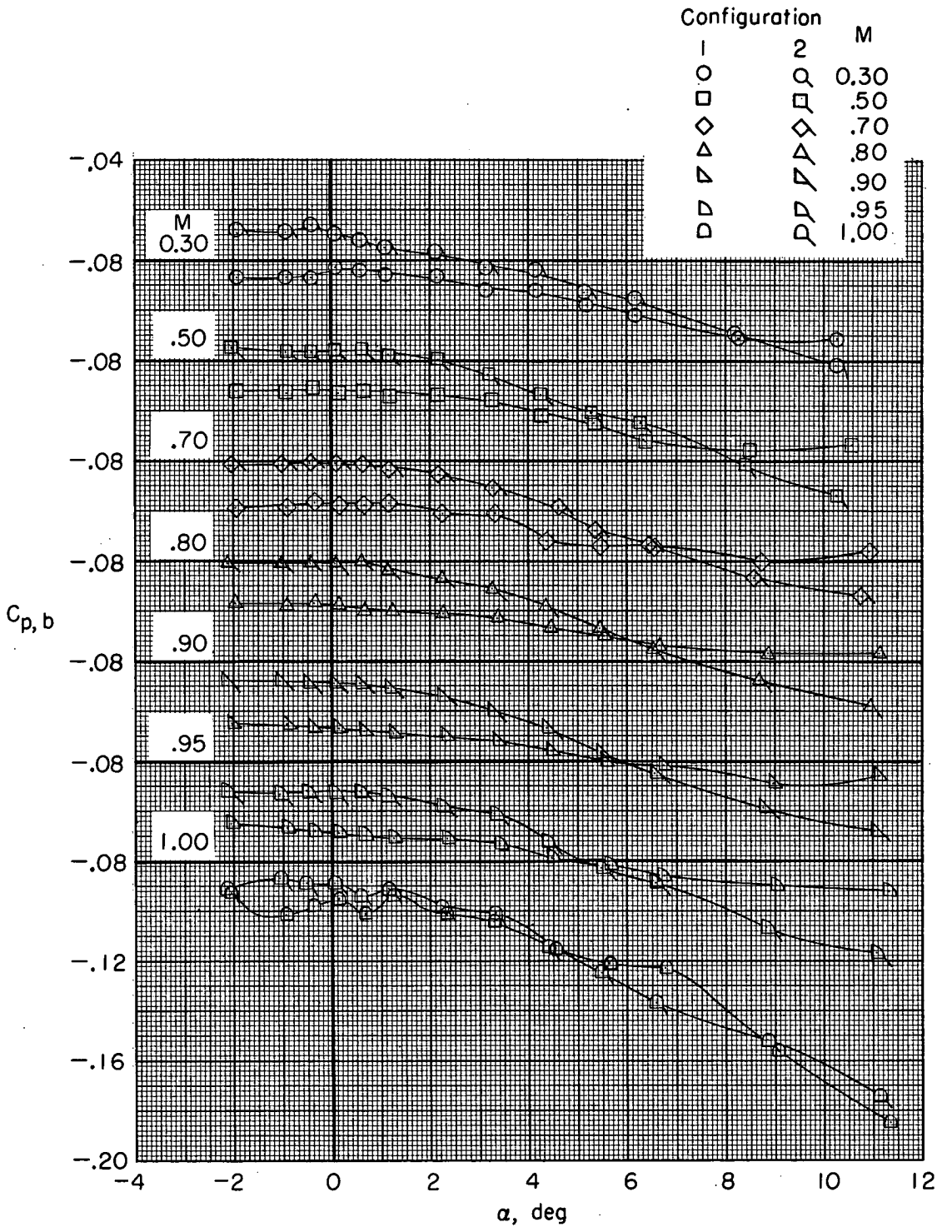

(a) M = 0.30 to 1.00.

Figure 4.- Variation of base pressure coefficient with angle of attack for both configurations at various Mach numbers.

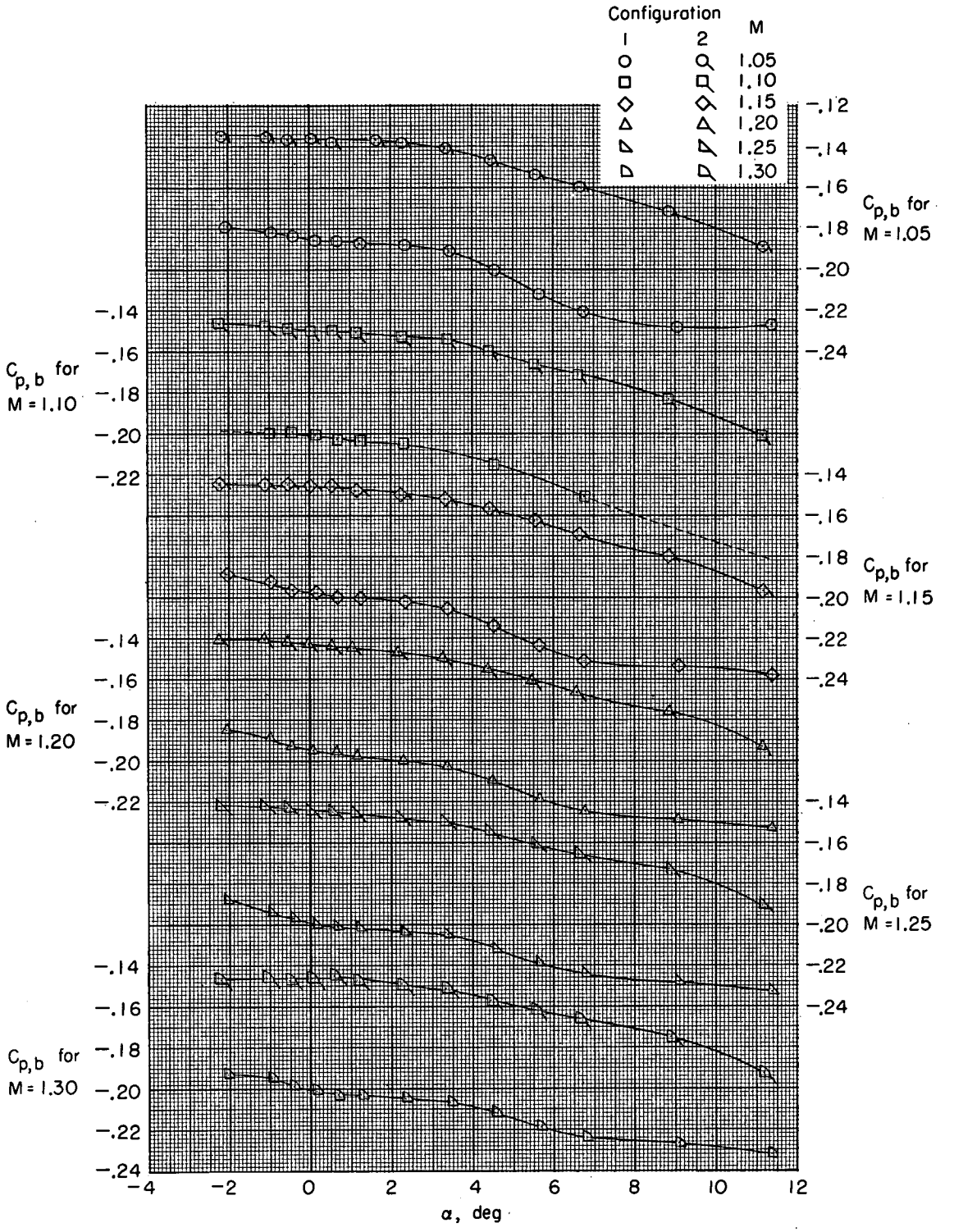

(b) M = 1.05 to 1.30.

Figure 4.- Concluded.

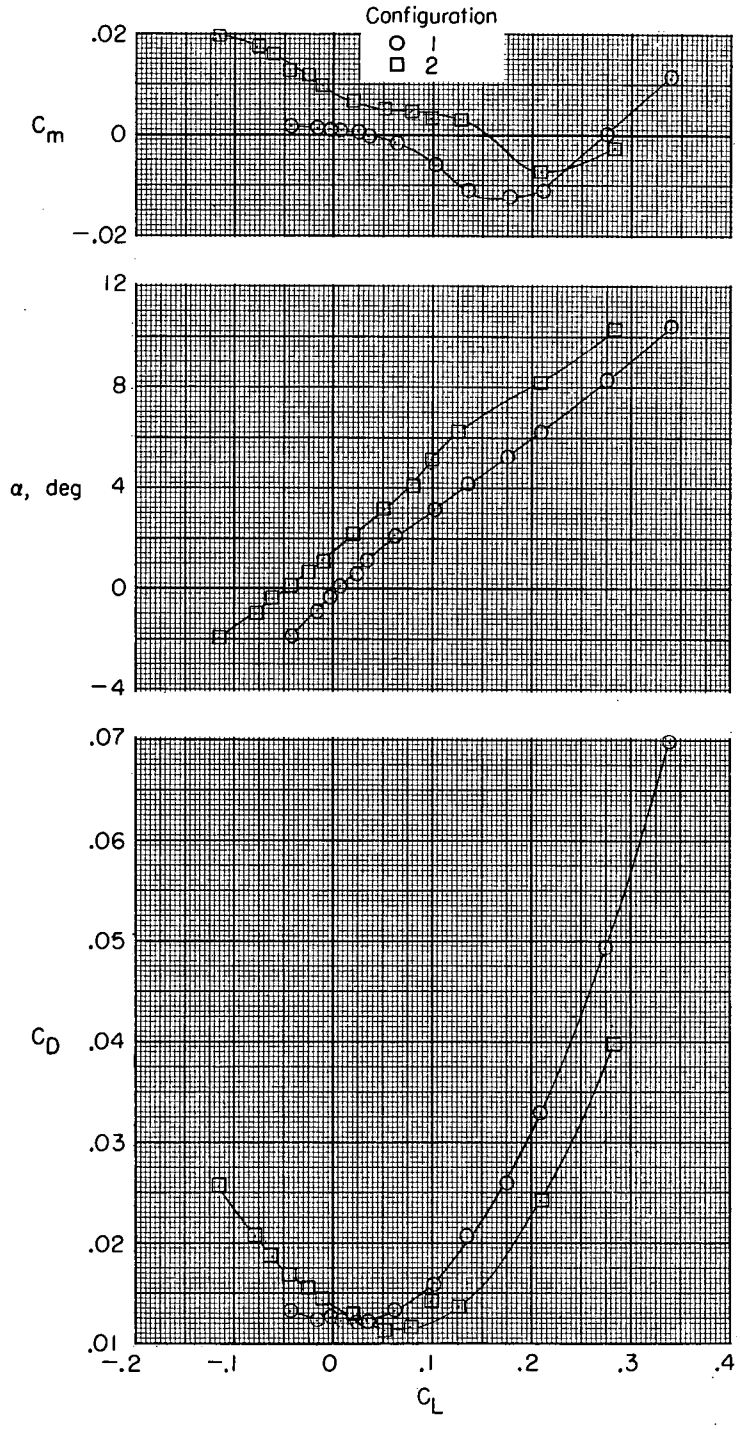

(a) M = 0.30.

Figure 5.- Longitudinal aerodynamic characteristics of the two configurations.

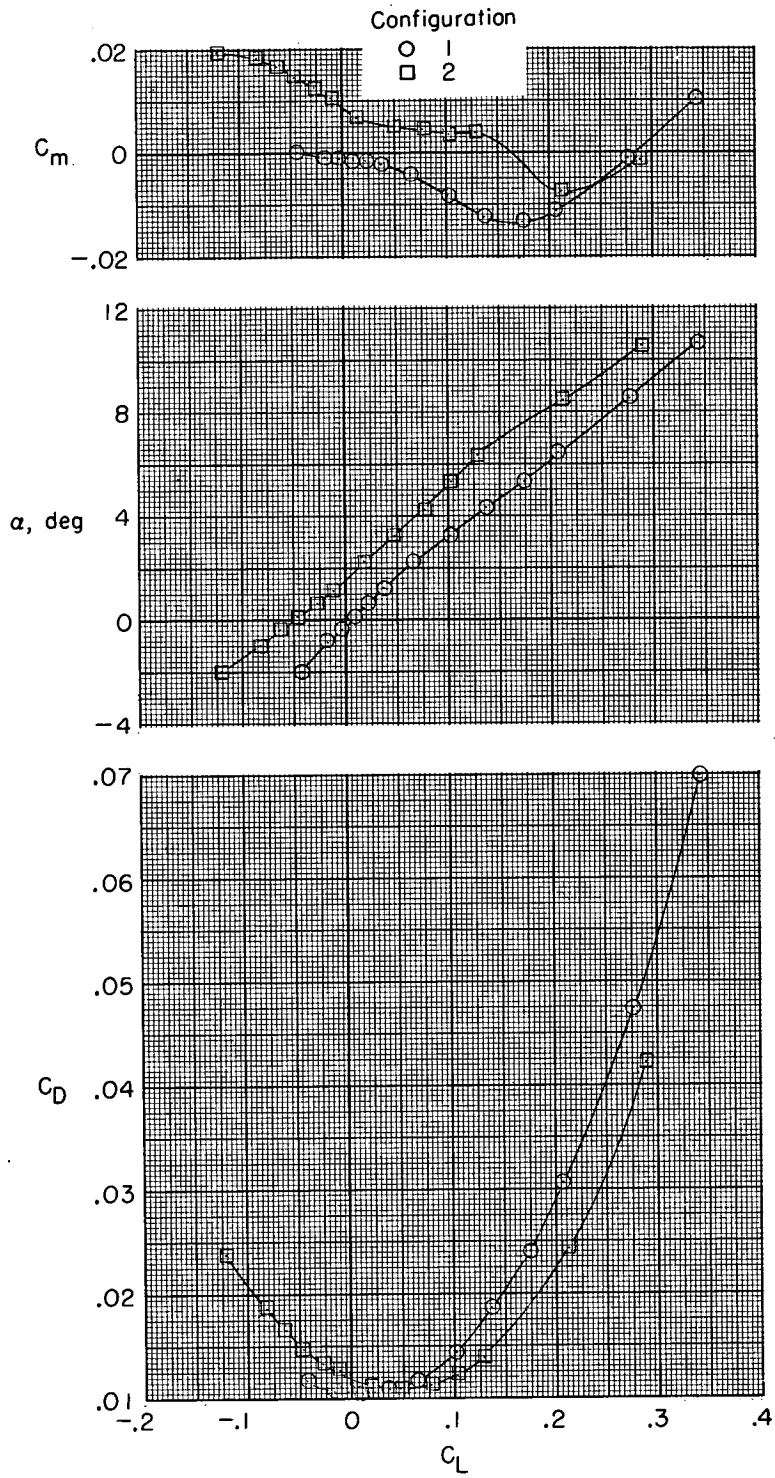

(b) M = 0.50.

Figure 5.- Continued.

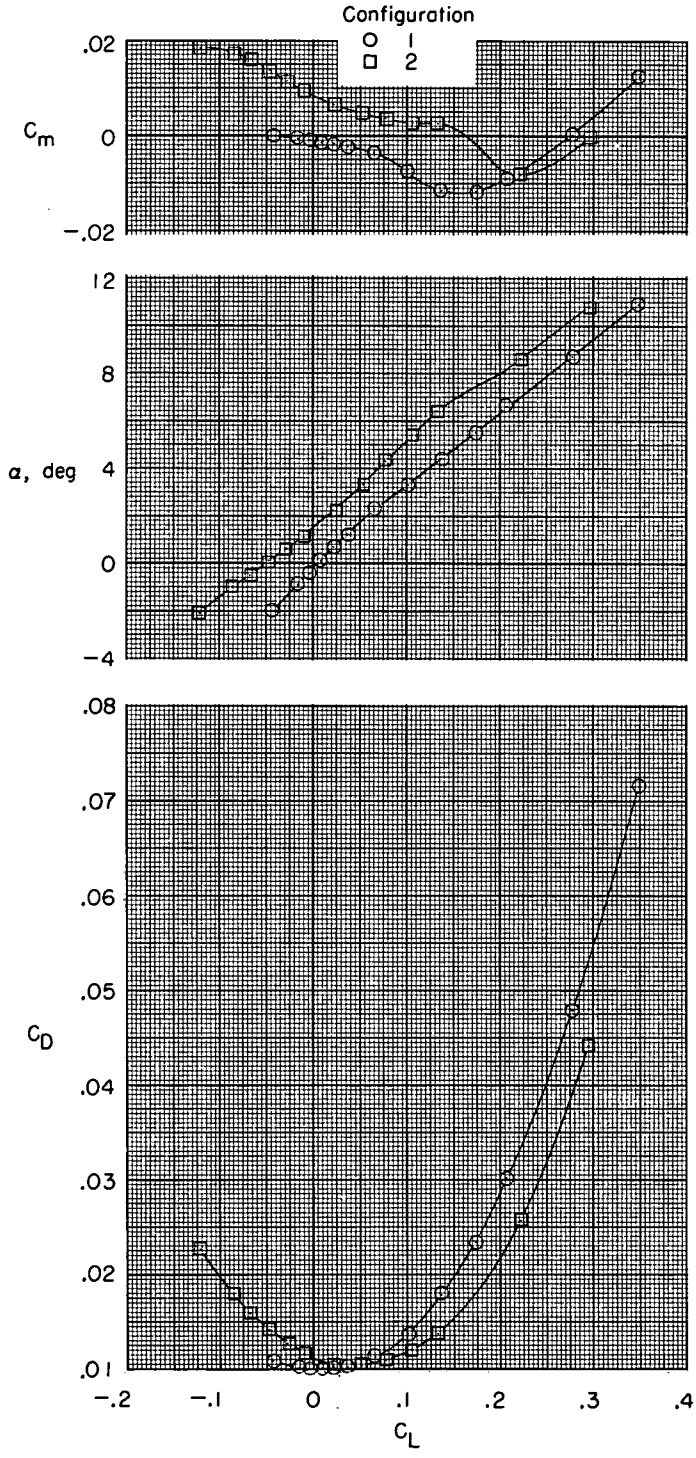

(c) M = 0.70.

Figure 5.- Continued.

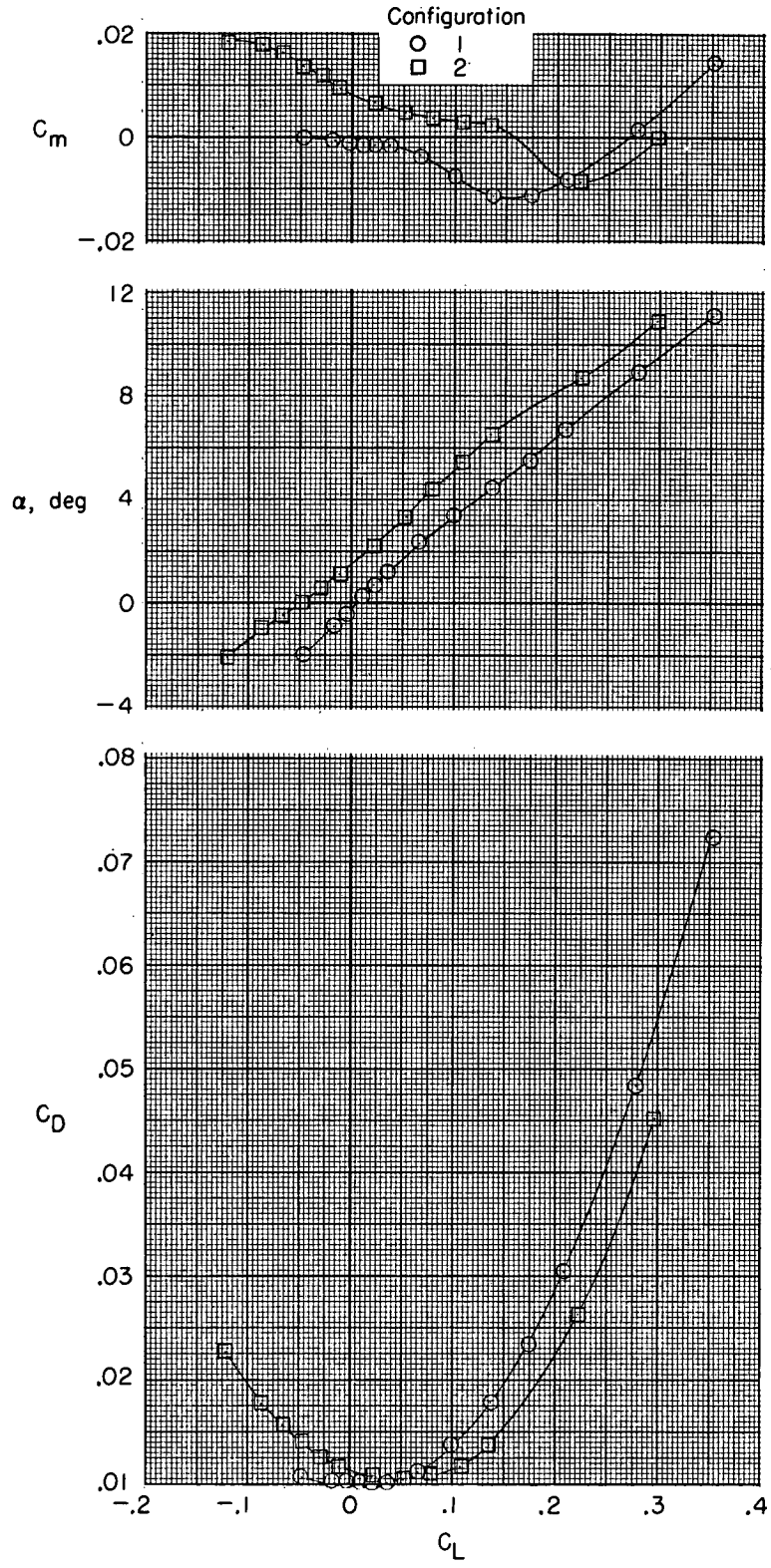

(d) M = 0.80.

Figure 5.- Continued.

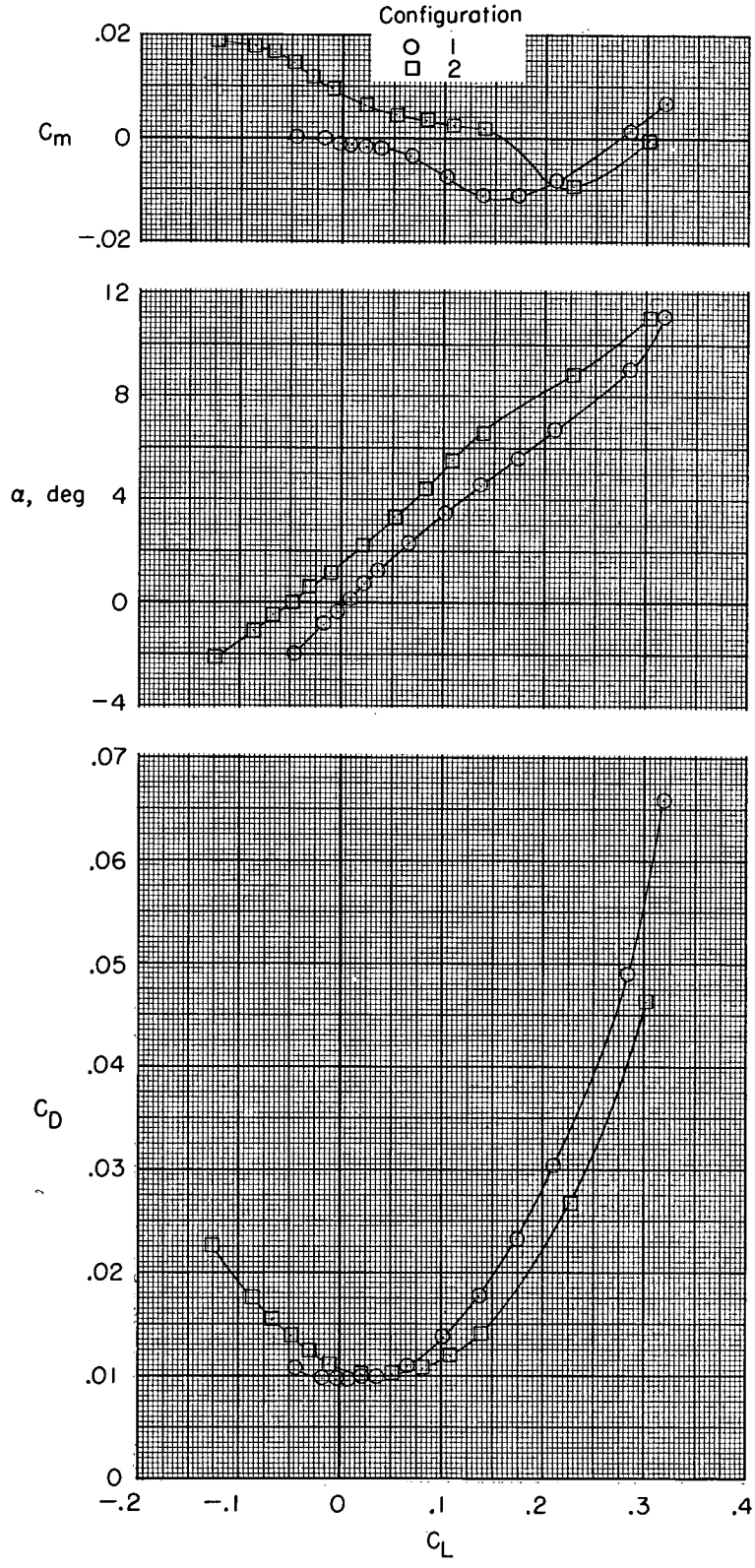

(e) M = 0.90.

Figure 5.- Continued.

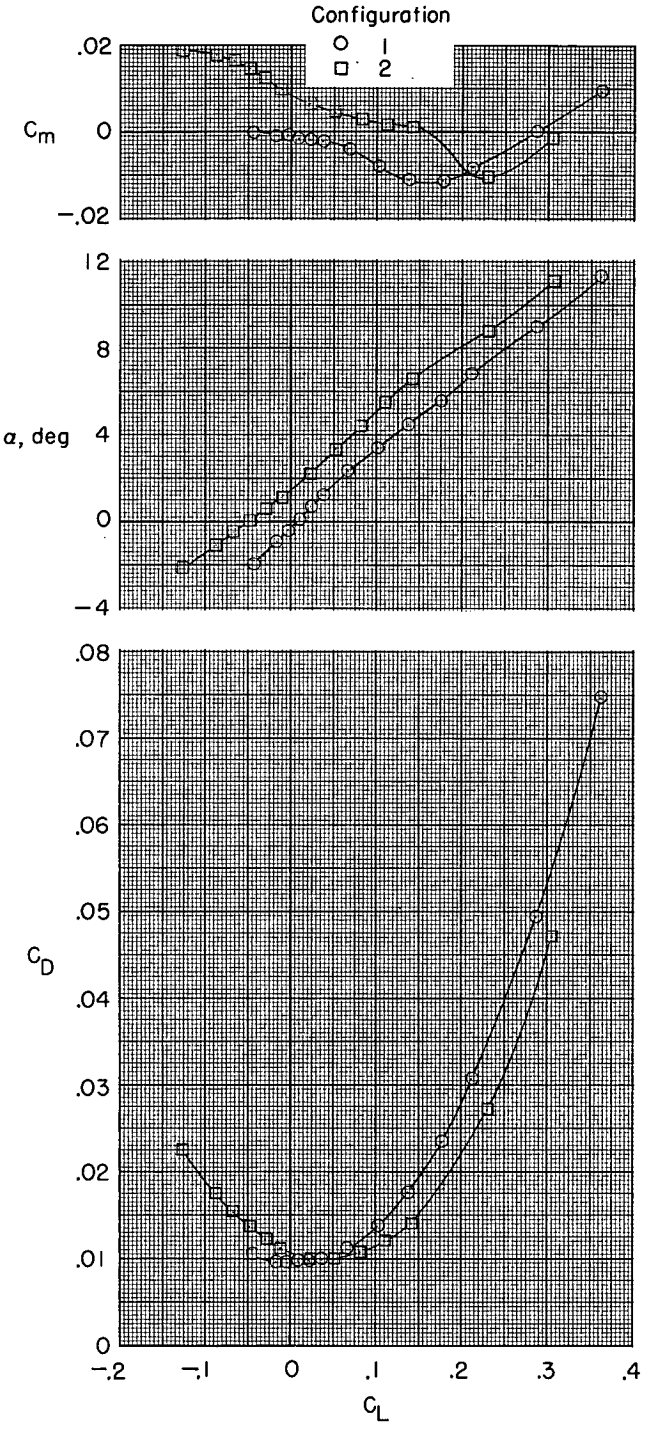

(f) M = 0.95.

Figure 5.- Continued.

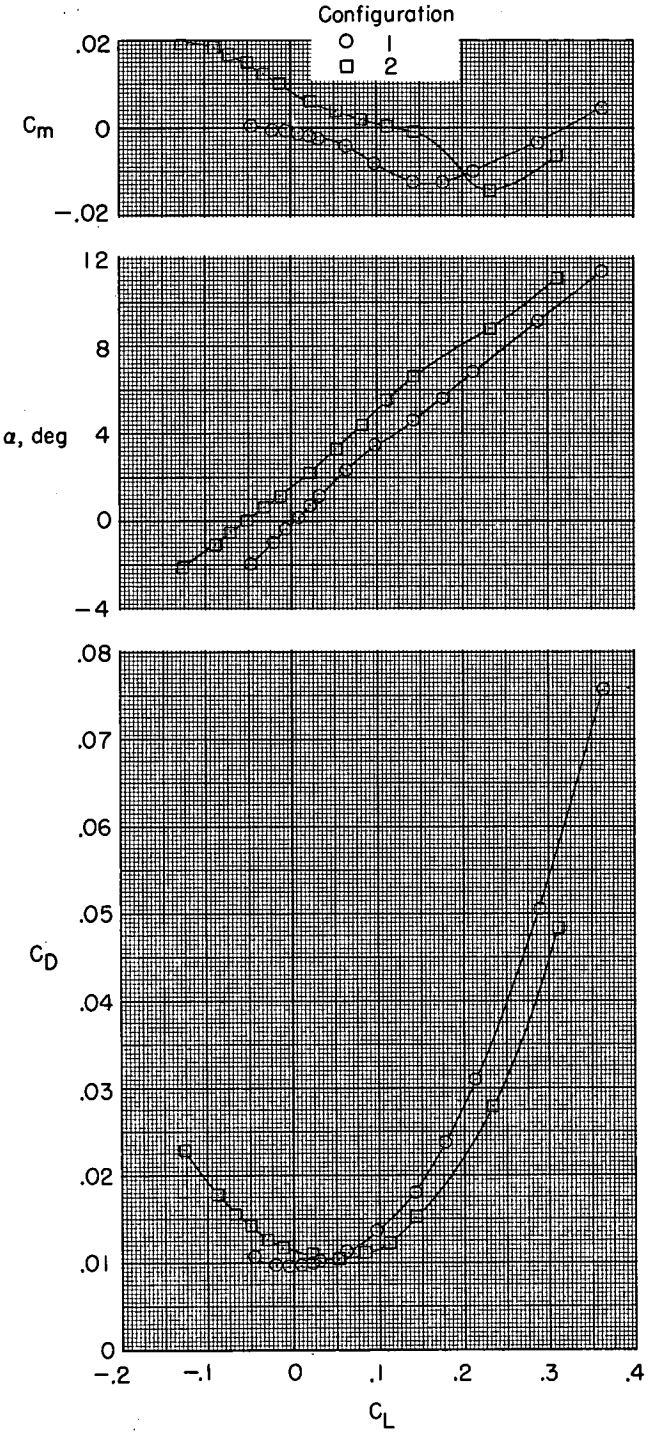

(g) M = 1.00.

Figure 5.- Continued.

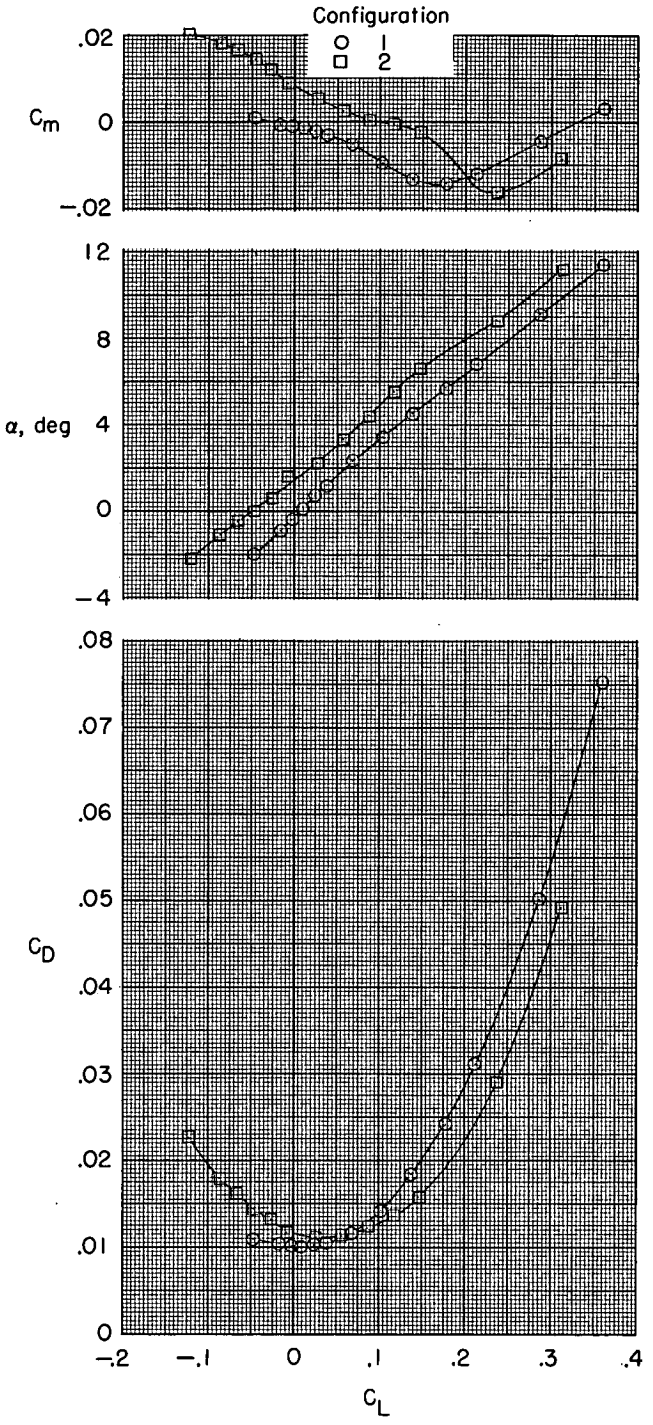

(h) M = 1.05.

Figure 5.- Continued.

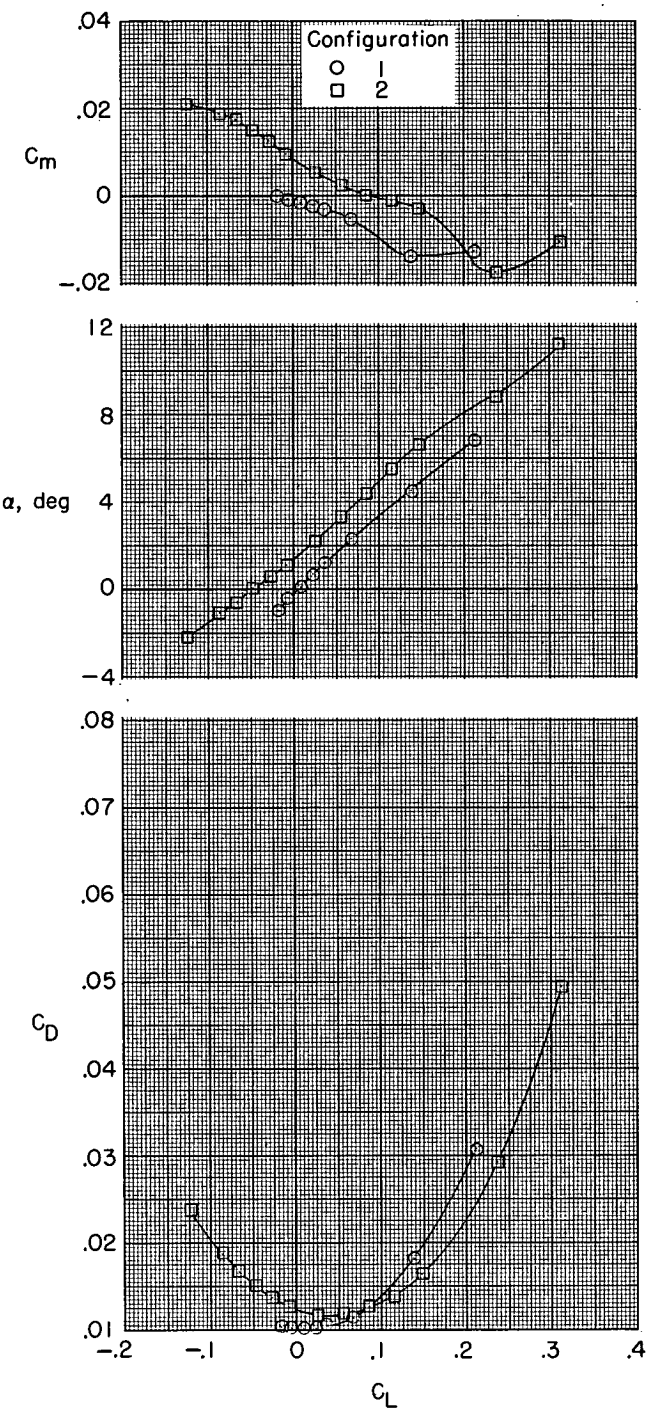

(i) M = 1.10.

Figure 5.- Continued.

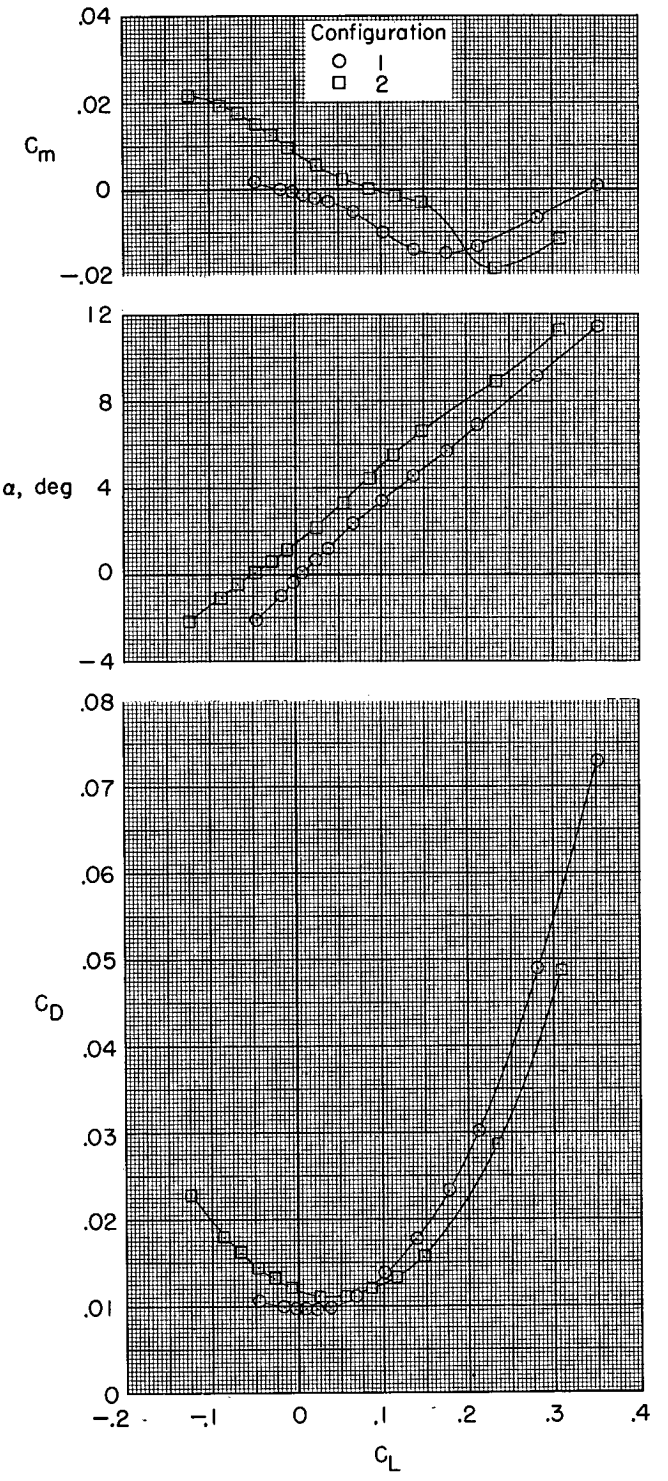

(j) M = 1.15.

Figure 5.- Continued.

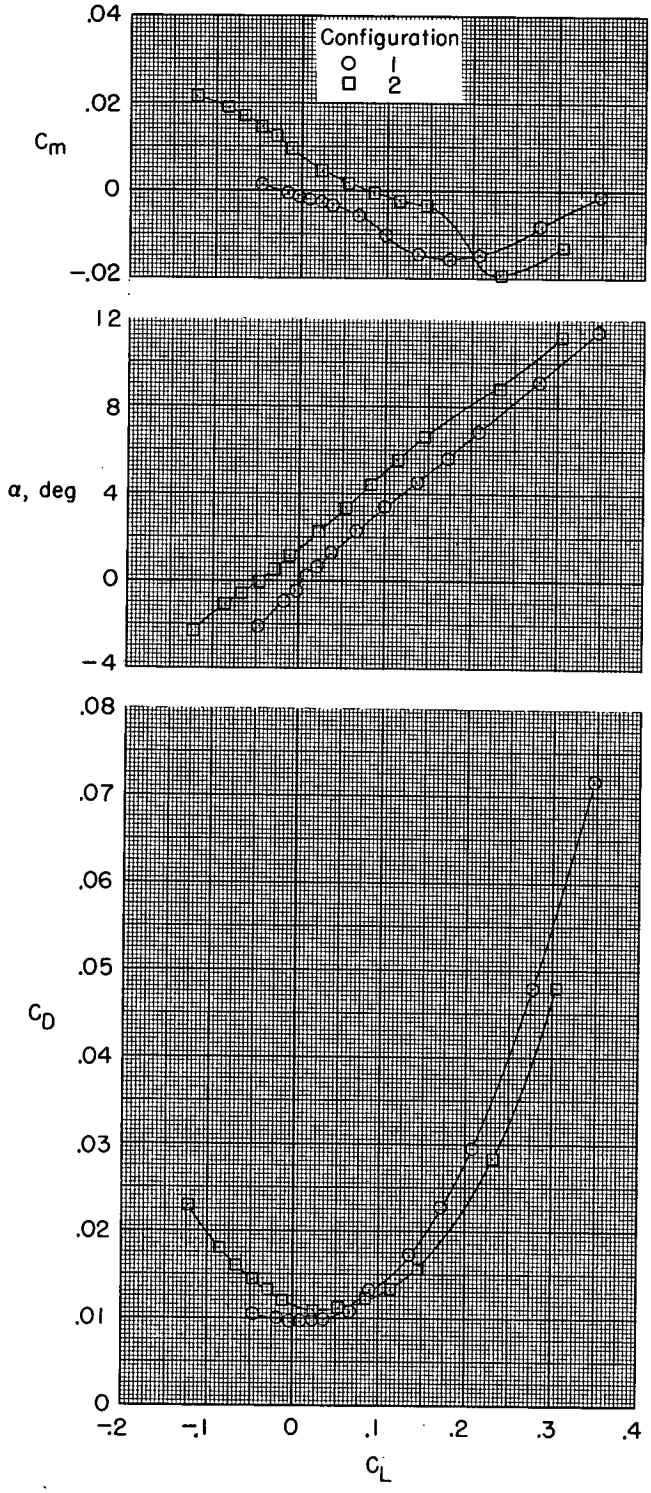

(k) M = 1.20.

Figure 5.- Continued.

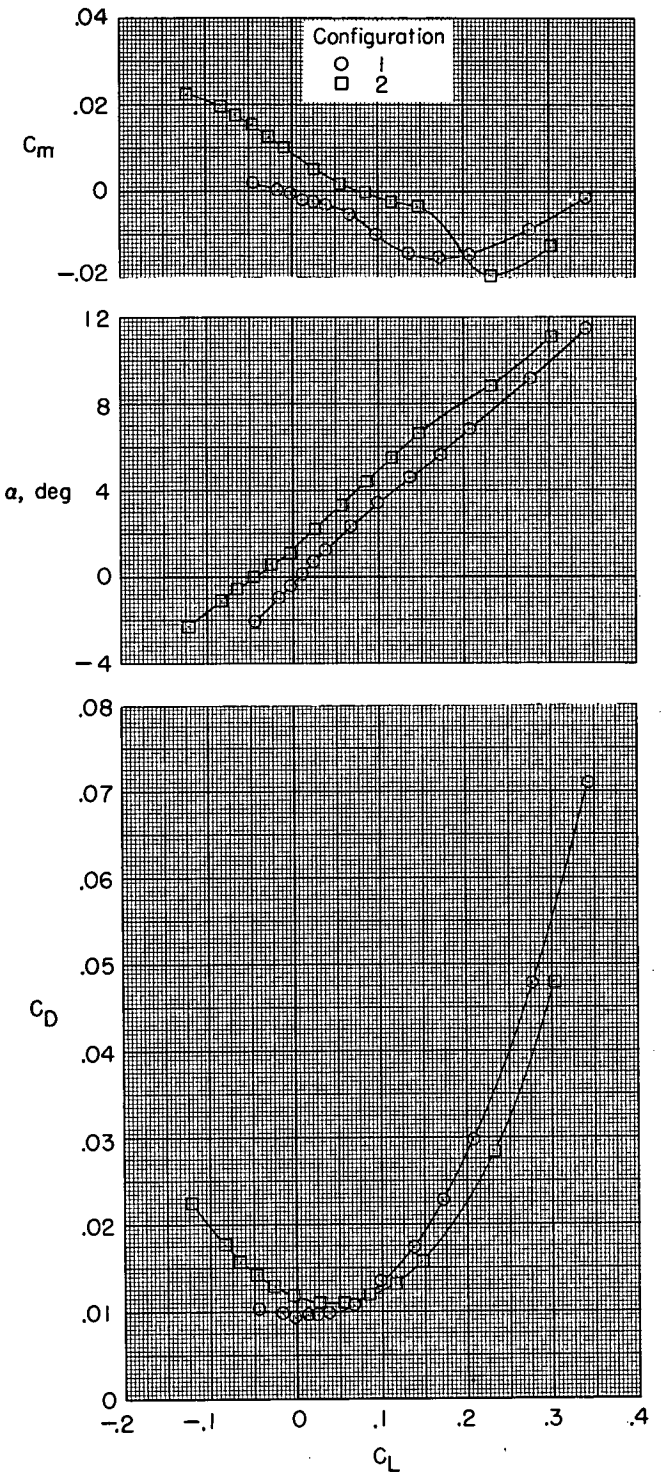

(l) M = 1.25.

Figure 5.- Continued.

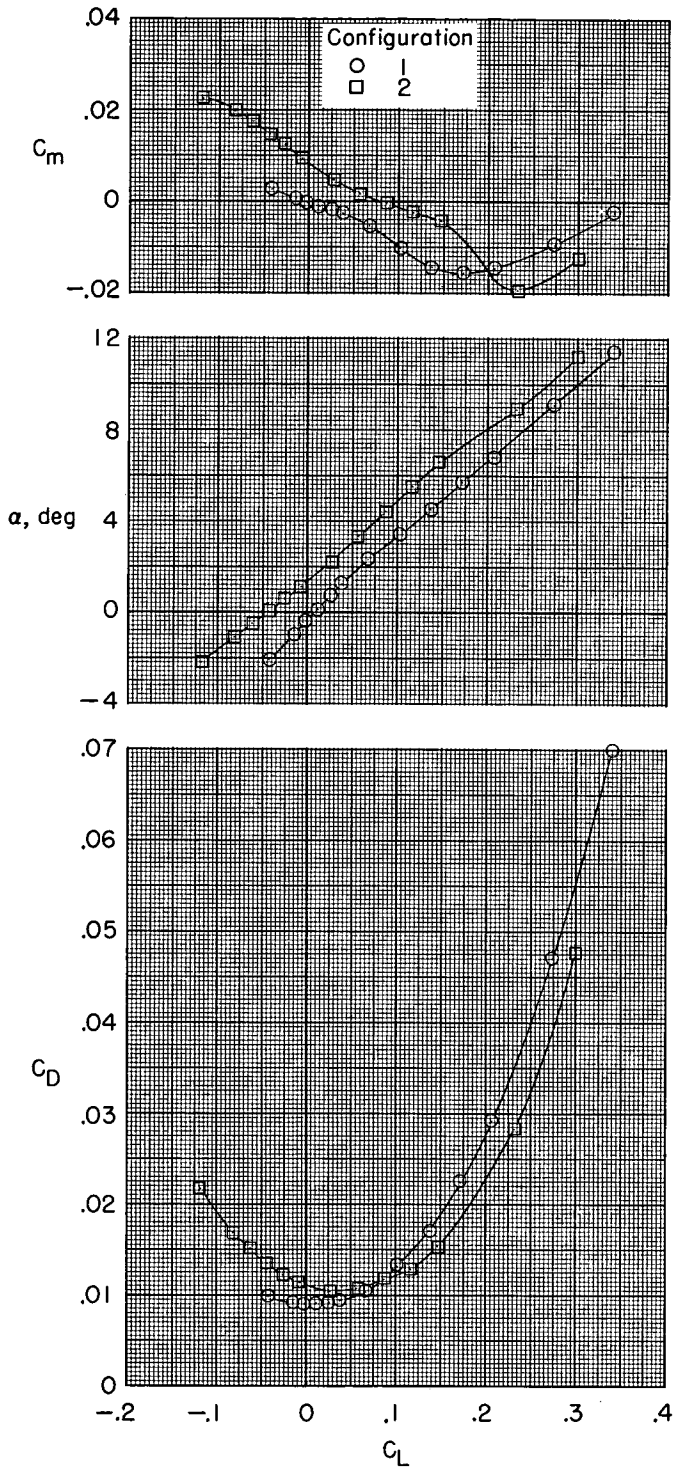

(m) M = 1.30.

Figure 5.- Concluded.

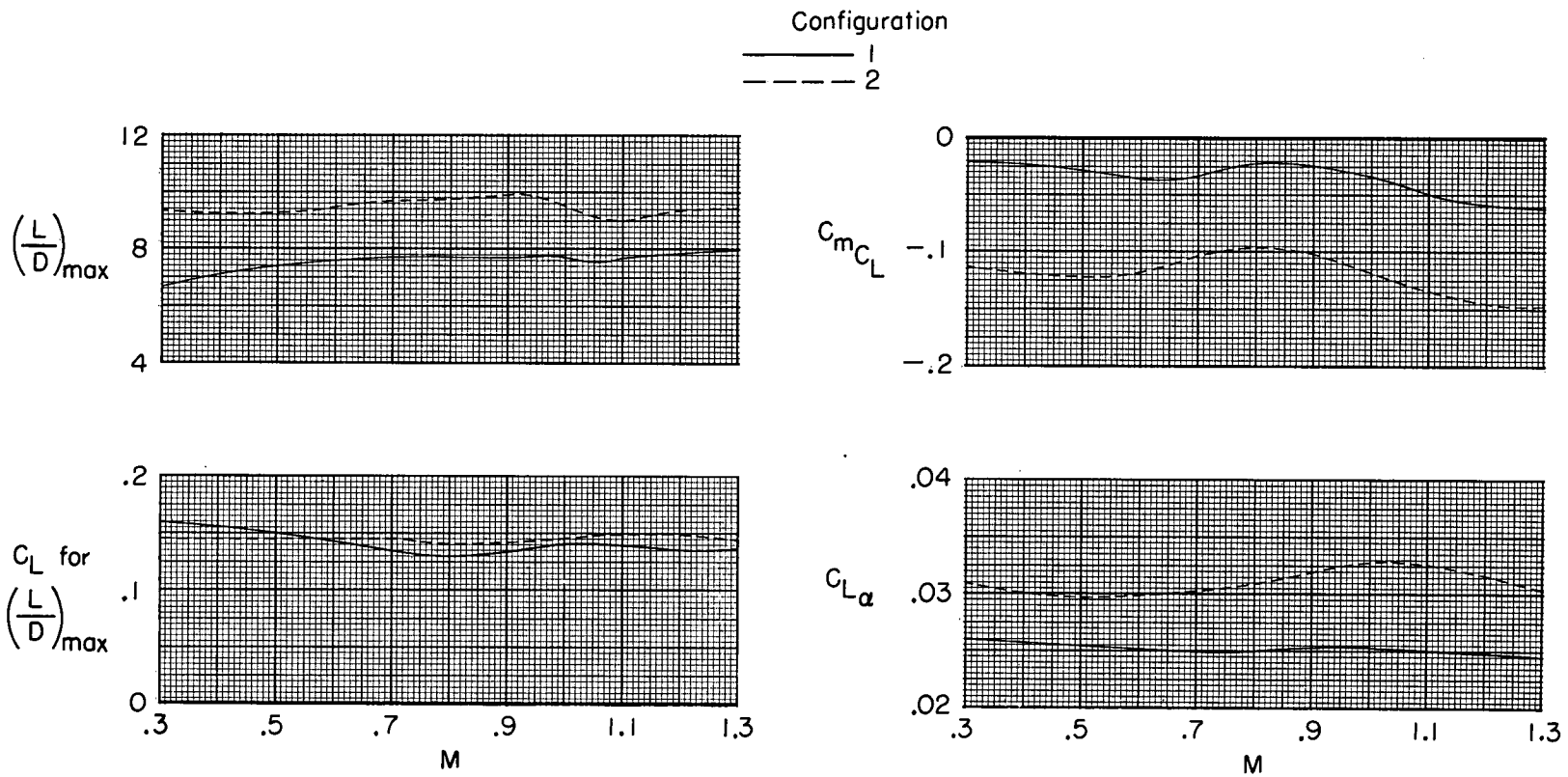

Figure 6.- Variation of $(L/D)_{max}$, C_L for $(L/D)_{max}$, $C_{m_{C_L}}$, and C_{L_α} with Mach number.

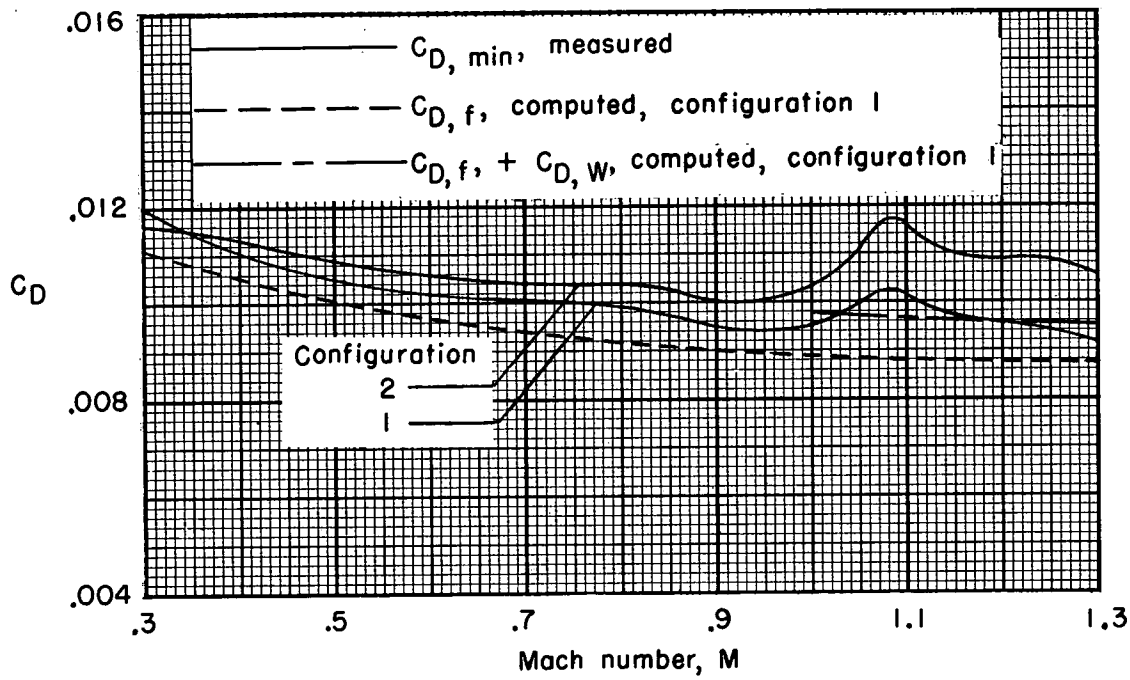

Figure 7.- Comparison of measured $C_{D,min}$ for both configurations with computed $C_{D,f}$ and $C_{D,f} + C_{D,W}$ for configuration 1.

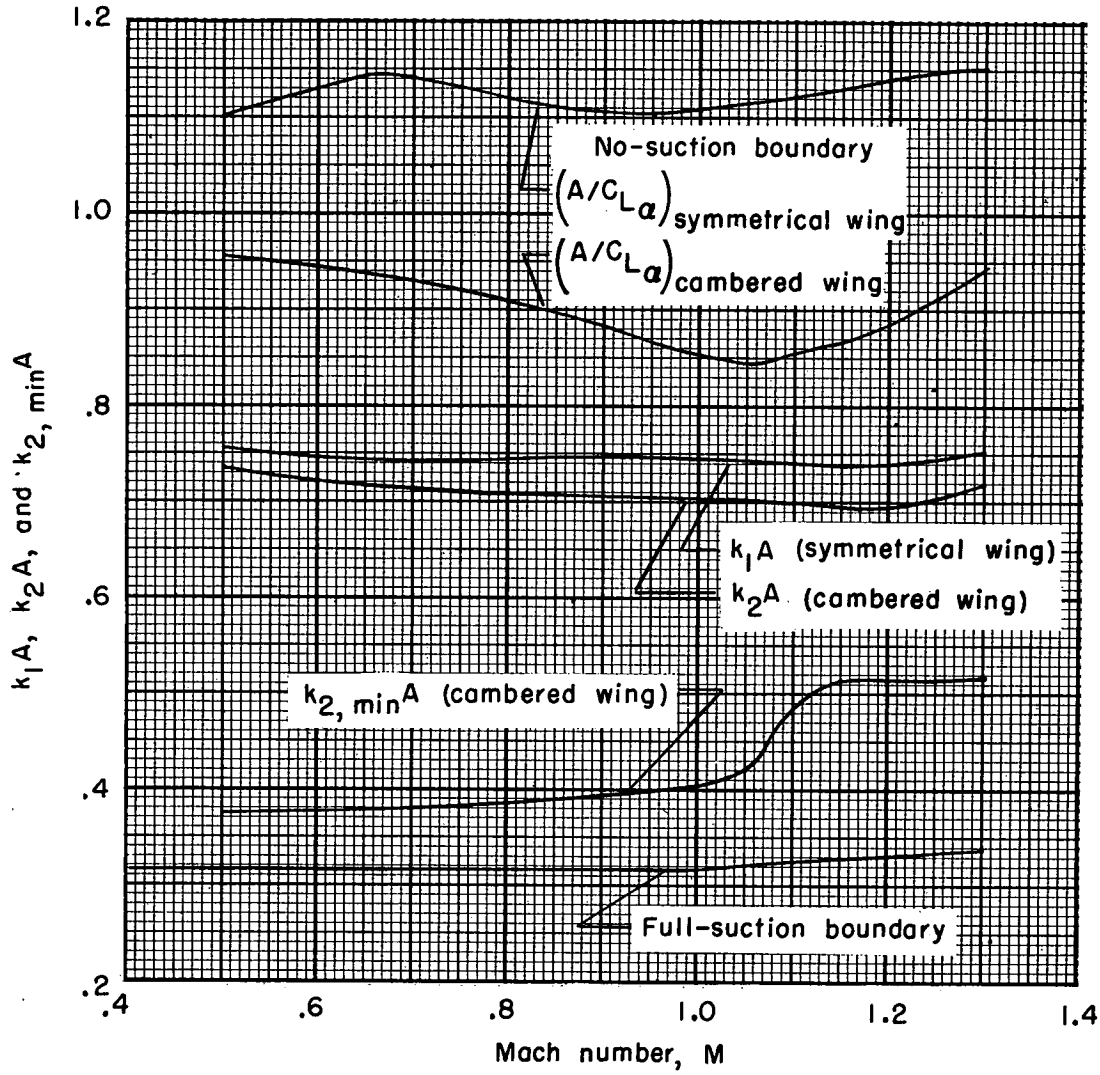

Figure 8.- Comparisons showing effects of leading-edge suction and span load efficiency on performance of the symmetrical-wing and cambered-wing configurations.

~~CONFIDENTIAL~~

"The aeronautical and space activities of the United States shall be conducted so as to contribute . . . to the expansion of human knowledge of phenomena in the atmosphere and space. The Administration shall provide for the widest practicable and appropriate dissemination of information concerning its activities and the results thereof."

—NATIONAL AERONAUTICS AND SPACE ACT OF 1958

NASA SCIENTIFIC AND TECHNICAL PUBLICATIONS

TECHNICAL REPORTS: Scientific and technical information considered important, complete, and a lasting contribution to existing knowledge.

TECHNICAL NOTES: Information less broad in scope but nevertheless of importance as a contribution to existing knowledge.

TECHNICAL MEMORANDUMS: Information receiving limited distribution because of preliminary data, security classification, or other reasons.

CONTRACTOR REPORTS: Scientific and technical information generated under a NASA contract or grant and considered an important contribution to existing knowledge.

TECHNICAL TRANSLATIONS: Information published in a foreign language considered to merit NASA distribution in English.

SPECIAL PUBLICATIONS: Information derived from or of value to NASA activities. Publications include conference proceedings, monographs, data compilations, handbooks, sourcebooks, and special bibliographies.

TECHNOLOGY UTILIZATION PUBLICATIONS: Information on technology used by NASA that may be of particular interest in commercial and other non-aerospace applications. Publications include Tech Briefs, Technology Utilization Reports and Notes, and Technology Surveys.

Details on the availability of these publications may be obtained from:

SCIENTIFIC AND TECHNICAL INFORMATION DIVISION

NATIONAL AERONAUTICS AND SPACE ADMINISTRATION

Washington, D.C. 20546

~~CONFIDENTIAL~~